

# Optical Engineering

OpticalEngineering.SPIEDigitalLibrary.org

## **Generating partially coherent Schell-model sources using a modified phase screen approach**

Milo W. Hyde, IV  
Santasri Basu  
David G. Voelz  
Xifeng Xiao

# Generating partially coherent Schell-model sources using a modified phase screen approach

Milo W. Hyde IV,<sup>a,\*</sup> Santasri Basu,<sup>b</sup> David G. Voelz,<sup>c</sup> and Xifeng Xiao<sup>c</sup>

<sup>a</sup>Air Force Institute of Technology, Department of Electrical and Computer Engineering, Dayton, 2950 Hobson Way Wright-Patterson AFB, Ohio 45433, United States

<sup>b</sup>Air Force Institute of Technology, Department of Engineering Physics, Dayton, 2950 Hobson Way Wright-Patterson AFB, Ohio 45433, United States

<sup>c</sup>New Mexico State University, Klipsch School of Electrical and Computer Engineering, Las Cruces, MSC 3-O, Goddard Annex 160B Las Cruces, New Mexico 88003, United States

**Abstract.** A significant improvement to the recently introduced complex screen (CS) method for generating partially coherent Schell-model sources is presented. The method, called the modified phase screen (MPS) technique, applies a deterministic amplitude and the phase portion of a CS to an initially coherent light source using a single phase-only spatial light modulator. The MPS technique, unlike the CS approach from which it is derived, does not produce a fully developed speckle pattern in the source plane, and therefore converges faster and more uniformly to the desired partially coherent source. The analytical development of the MPS method is presented. Experimental results of a Bessel-Gaussian-correlated Schell-model source, generated using the CS and MPS approaches, are compared to demonstrate the validity and utility of the MPS technique. © The Authors. Published by SPIE under a Creative Commons Attribution 3.0 Unported License. Distribution or reproduction of this work in whole or in part requires full attribution of the original publication, including its DOI. [DOI: 10.1117/1.OE.54.12.120501]

Keywords: coherence; speckle; statistical optics; spatial light modulators.

Paper 151387L received Oct. 3, 2015; accepted for publication Nov. 16, 2015; published online Dec. 10, 2015.

## 1 Introduction

Research into the nature of partially coherent light is quite popular. Much work has been performed predicting the behavior of partially coherent light as it propagates, traverses random media, and scatters from deterministic and random objects.<sup>1,2</sup> Controlling the coherence of light can provide significant advantages in such applications as free-space optical communications, remote sensing, directed energy, particle trapping, medicine, and manufacturing.

Considering the numerous possible benefits of exploiting coherence in optical applications, techniques to experimentally synthesize partially coherent beams/sources have followed.<sup>1,2</sup> Much of this synthesis research has focused on

generating Gaussian Schell-model (GSM) sources and their many variants. To achieve this, researchers commonly use a phase-only spatial light modulator (SLM) in combination with a Gaussian amplitude filter.<sup>1,2</sup> This approach has two main drawbacks. The first is that the system lacks flexibility, i.e., producing a GSM source with a different Gaussian amplitude width requires a new filter. Of course, this requirement also applies to Schell-model sources with general amplitudes.

The second drawback is that one is practically limited to producing sources with coherence functions belonging to the power exponential family, of which the Laplacian and Gaussian functions are the most popular members.<sup>3</sup> This is not a significant shortcoming if one is interested in producing only GSM sources; however, it is debilitating if one desires to produce general Schell-model sources. This drawback comes from using Gaussian random numbers to generate GSM phase screens that are subsequently commanded to the SLM. This is discussed in detail in Ref. 4 and summarized below.

Recently, a technique to experimentally generate a general Schell-model source was introduced.<sup>4</sup> The method uses a single phase-only SLM to produce complex phase screens [complex screens (CS), hereafter], i.e., screens that impart changes to both the amplitude and phase of an initially coherent light source. Using this approach, any desired Schell-model source can be produced. Furthermore, because no amplitude filters are required and one can produce a source with any desired coherence function, the drawbacks mentioned previously are no longer applicable.

Although, in theory, any Schell-model source can be produced using the CS technique, in practice, because the resulting source fields are fully developed speckle patterns, many realizations are required to converge to the desired partially coherent source.<sup>4</sup>

Here, an improvement to the CS approach presented in Ref. 4 is introduced. Similar to the concept presented in Ref. 5, the new technique uses only the phase portion of the CS; however, unlike in Ref. 5, here the amplitude of the source is also controlled. This permits any desired Schell-model source to be produced. The new approach, called the modified phase screen (MPS) approach hereafter, does not produce fully developed speckle patterns in the source plane and therefore is much quicker to converge to the desired partially coherent source.

The analytical development of the MPS method is presented below. Included in this development are the germane details of the CS approach and how amplitude is controlled using a single phase-only SLM. Experimental results of a Bessel-Gaussian-correlated Schell-model (BGSM) source are presented to validate the new technique. Lastly, this paper concludes with a summary of the presented work and a brief discussion of contributions.

## 2 Methodology

### 2.1 Complex Screen Method

A general Schell-model source takes the form

$$W(\mathbf{p}_1, \mathbf{p}_2) = \langle U(\mathbf{p}_1)U^*(\mathbf{p}_2) \rangle = \sqrt{S(\mathbf{p}_1)}\sqrt{S(\mathbf{p}_2)}\mu(\mathbf{p}_1 - \mathbf{p}_2), \quad (1)$$

\*Address all correspondence to: Milo W. Hyde, E-mail: [milo.hyde@afit.edu](mailto:milo.hyde@afit.edu)

where  $W$  is the cross-spectral density function,  $U$  is the scalar optical field,  $S$  is the spectral density,  $\mu$  is the spectral degree of coherence, and  $\boldsymbol{\rho} = \hat{x}x + \hat{y}y$ .<sup>1</sup> Note that  $W$ ,  $U$ ,  $S$ , and  $\mu$  are, in general, functions of wavelength; this dependence is omitted for brevity.

A single instance of a CS field takes the form

$$U(\boldsymbol{\rho}) = \sqrt{S(\boldsymbol{\rho})}T(\boldsymbol{\rho}), \quad (2)$$

where  $T$  is the CS and is a sample function drawn from a zero-mean, circular complex Gaussian random process.<sup>4</sup> Taking the autocorrelation of Eq. (2) and comparing that result to Eq. (1) reveals that

$$\langle T(\boldsymbol{\rho}_1)T^*(\boldsymbol{\rho}_2) \rangle = \mu(\boldsymbol{\rho}_1 - \boldsymbol{\rho}_2). \quad (3)$$

Thus, any Schell-model source can be produced using the CS method if  $\langle |U|^2 \rangle = S$  and if a  $T$  can be synthesized with an autocorrelation equal to  $\mu$ . The latter is quite easy to do using the method described in Ref. 4.

Note that the CS approach produces a fully developed speckle pattern in the source plane. This can be shown by computing the speckle contrast<sup>6</sup>

$$C(\boldsymbol{\rho}) = \sqrt{\frac{\langle |U(\boldsymbol{\rho})|^4 \rangle - \langle |U(\boldsymbol{\rho})|^2 \rangle^2}{\langle |U(\boldsymbol{\rho})|^2 \rangle^2}}, \quad (4)$$

where  $\langle |U|^2 \rangle = S$ . The fourth moment of  $U$  can be found by applying the complex Gaussian moment theorem<sup>6</sup> (recall that  $T$  is circular complex Gaussian) yielding  $\langle |U|^4 \rangle = 2S^2$ . Substituting these moments into Eq. (4) produces  $C = 1$ .

## 2.2 Modified Phase Screen Method

For the MPS technique,  $U = \sqrt{S} \exp(j\phi)$ , where  $\phi$  is a sample function drawn from a zero-mean, real random process. Taking the autocorrelation of  $U$  and comparing that expression to Eq. (1) reveals the equalities

$$\chi(\boldsymbol{\rho}_1, \boldsymbol{\rho}_2) = \langle e^{j\phi(\boldsymbol{\rho}_1)} e^{-j\phi(\boldsymbol{\rho}_2)} \rangle = \mu(\boldsymbol{\rho}_1 - \boldsymbol{\rho}_2). \quad (5)$$

To the authors' knowledge, the right-side condition, in general, cannot be met.<sup>5</sup> If one generates  $\phi$  in the traditional way, i.e., using Gaussian random numbers, then

$$\chi(\boldsymbol{\rho}_1, \boldsymbol{\rho}_2) = \exp\{-\sigma_\phi^2[1 - \gamma(\boldsymbol{\rho}_1 - \boldsymbol{\rho}_2)]\}, \quad (6)$$

where  $\sigma_\phi^2$  is the variance of  $\phi$  and  $\gamma$  is the normalized autocorrelation function of  $\phi$  (note that  $|\gamma| \leq 1$ ).

Other than producing sources with power-exponential-type  $\mu$ , little else can be done with Eq. (6). For instance, assume that a Schell-model source with a triangular-shaped spectral degree of coherence  $\mu = \Lambda$  is desired. Inverting Eq. (6) yields  $\gamma = 1 + \ln \Lambda / \sigma_\phi^2$ . Note that the  $|\gamma| \leq 1$  condition is violated when the triangle function  $\Lambda = 0$ . Therefore, producing a source with a triangular  $\mu$ , as well as most other shapes, is not possible using traditional Gaussian phase screens.

As alluded to above, the only thing that can practically be done with Eq. (6) is to produce sources with  $\mu$  belonging to the power exponential family. To do this, one assumes that  $\sigma_\phi^2 \gg 1$ , thereby requiring that  $\gamma \approx 1$  for  $\chi$  to possess an appreciable value. Expanding  $\gamma$  in a Maclaurin series and

keeping the first two terms yields Schell-model sources with power-exponential-type coherence functions.<sup>4</sup>

Although Eq. (5) cannot be satisfied in general,  $\chi \approx \mu$  if  $\phi = \arg(T)$ . This can be shown by numerically computing  $\chi$  using the joint probability density function of speckle phases

$$\chi = \int_{-\pi}^{\pi} \int_{-\pi}^{\pi} \exp[j(\phi_1 - \phi_2)] \left( \frac{1 - |\mu|^2}{4\pi^2} \right) \times \frac{\sqrt{1 - \beta^2} + \pi\beta - \beta \cos^{-1}\beta}{(1 - \beta^2)^{3/2}} d\phi_1 d\phi_2, \quad (7)$$

where  $\beta = |\mu| \cos[\arg(\mu) + \phi_1 - \phi_2]$ .<sup>6</sup> Comparing Eq. (7) to  $\mu$  for all values of  $|\mu| \in [0, 1]$  and  $\arg(\mu) \in (-\pi, \pi]$  reveals that  $\chi \approx \mu$  if  $\phi = \arg(T)$ . The interested reader is referred to Ref. 5 for more details about this result.

Thus, an instance of an MPS field takes the form

$$U(\boldsymbol{\rho}) = \sqrt{S(\boldsymbol{\rho})} \exp\{j \arg[T(\boldsymbol{\rho})]\}, \quad (8)$$

where  $T$  is produced using the approach described in Ref. 4. In contrast to the CS approach, the MPS method does not yield a fully developed speckle pattern in the source plane. Again, this can be shown by computing the speckle contrast. Here,  $\langle |U|^2 \rangle = S$  and  $\langle |U|^4 \rangle = S^2$ . Substituting these into Eq. (4) produces  $C = 0$ .

Because it does not produce fully developed speckle patterns in the source plane, the MPS method converges more quickly and uniformly to the desired Schell-model source than does the CS approach. This is demonstrated in the experimental results to follow. Recall, however, that the MPS method does not yield the exact  $\mu$  as opposed to the CS approach ( $\chi \approx \mu$ ). The difference between  $\chi$  and  $\mu$  is very slight, such that the produced Schell-model source is practically indistinguishable from the desired partially coherent source.<sup>5</sup>

Reference 5 used the MPS approach to produce any desired mean, far-zone irradiance pattern. No consideration was given to the amplitude of the field in the source plane (i.e.,  $\sqrt{S}$ ), which predominately drives  $\mu$  in the far zone.<sup>1</sup> Producing a source-plane field  $U$  with an amplitude equal to  $\sqrt{S}$  using a single phase-only SLM is easily accomplished by using the SLM to create a periodic sawtooth phase grating that produces the desired  $U$  in the first diffraction order. Through careful manipulation of the characteristics of the grating, both the amplitude and phase of  $U$  can be precisely controlled.

The expression relating the sawtooth grating characteristics (its height and period) to the amplitude and phase of the field in the first diffraction order has been derived previously.<sup>4,7,8</sup> As was done in those references, using the physical optics approximation and assuming that more than four SLM pixels comprise each sawtooth, the approximate relation between sawtooth height and the field in the first diffraction order is found to be

$$U(\boldsymbol{\rho}) \propto \text{sinc}\{\pi[1 - h(\boldsymbol{\rho})]\} \exp\{-j\pi[1 - h(\boldsymbol{\rho})]\}, \quad (9)$$

where  $h$  is the sawtooth height in waves and  $\text{sinc}(x) = \sin(x)/x$ .

Forming an instance of an MPS field is simply a matter of

1. choosing a desired  $S$ ,

2. solving  $h = 1 - (1/\pi)\text{sinc}^{-1}(\sqrt{S})$ ,
3. forming the two-dimensional sawtooth grating with the appropriate  $h$ ,
4. applying the two-dimensional phase correction  $\exp[j\pi(1-h)]$  (i.e., the unwanted phase caused by the grating), and
5. applying the two-dimensional desired phase  $\phi = \arg(T)$ .

The desired field  $U$  appears in the first diffraction order.

As implied by the dependence of  $h$  on  $\rho$  in Eq. (9), the heights of the sawteeth making up the grating do, in general, vary; however, all the sawteeth contain the same number of SLM pixels. The grating can be formed in the horizontal, vertical, or in both directions. The number of pixels per sawtooth determines the fidelity of  $|U|$  (more is better) and the relative separation of the diffraction orders (fewer pixels provides greater separation). Thus, the number of pixels per sawtooth must be chosen such that an accurate  $|U|$  can be generated while providing enough separation between diffraction orders so that the desired first order can be isolated from the others (typically using a spatial filter) with minimal corruption.

### 3 Experimental Results

Figure 1 shows a schematic of the experimental setup. Note that this is the same setup that was used in Ref. 4; thus, only the important details are provided here.

The apparatus shown in Fig. 1 is designed to capture both the source-plane and far-zone irradiance patterns simultaneously. It is clear from Eq. (1) that the source-plane  $S$  can be obtained by measuring the source-plane irradiance. Thus, the images collected by the source-plane camera (SPC) assess

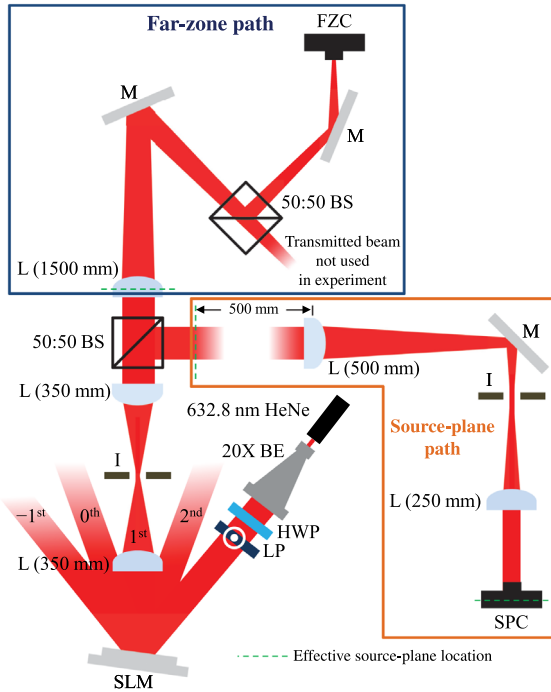


**Fig. 1** Schematic of the experimental setup—BE, beam expander; HWP, half-wave plate; LP, linear polarizer; SLM, spatial light modulator; L, lens; I, iris; BS, beam splitter; M, mirror; FZC, far-zone camera; and SPC, source-plane camera.

how well the MPS technique produces the desired Schell-model source's spectral density. Furthermore, it can be shown that the far-zone  $S$  is predominately driven by the source-plane  $\mu$ .<sup>1</sup> Thus, the images collected by the far-zone camera (FZC) assess how well the MPS technique produces the desired Schell-model source's spectral degree of coherence.

In the experimental results to follow, 5000 SPC and FZC images were used to compute the source-plane and far-zone spectral densities. Eight pixels per sawtooth were used to form the sawtooth grating. This number produced an accurate  $|U|$  while separating the diffraction orders enough such that a spatial filter could easily isolate the desired first order. The grating was formed in both the horizontal and vertical directions to move the first diffraction order away from the bright-side lobes (oriented in the horizontal and vertical directions) of the zeroth order.<sup>4</sup>

Figure 2 shows the theoretical, experimental CS, and experimental MPS results for a BGSM source. The cross-spectral density function for a BGSM source takes the form

$$W(\rho_1, \rho_2) = \exp\left(-\frac{\rho_1^2 + \rho_2^2}{4\sigma^2}\right) J_0\left(\frac{\beta}{\delta} |\rho_1 - \rho_2|\right) \exp\left(-\frac{|\rho_1 - \rho_2|^2}{2\delta^2}\right), \quad (10)$$

where  $\sigma$  and  $\delta$  are the root-mean-square widths of the spectral density and the Gaussian component of the spectral degree of coherence, respectively;  $\beta$  is a real constant; and  $J_0$  is a zeroth-order Bessel function of the first kind.<sup>1</sup> The BGSM cross-spectral density function measured by the FZC is

$$W(\rho_1, \rho_2) = \frac{k^2 \sigma^2}{2\gamma f^2} \exp\left(-\frac{\beta^2}{4\gamma \delta^2}\right) \exp\left[\frac{jk}{2f}(\rho_1^2 - \rho_2^2)\right] \times \exp\left[-\frac{1}{16\gamma} \left|\frac{k}{f}(\rho_1 + \rho_2)\right|^2\right] I_0\left[\frac{\beta}{4\gamma \delta} \left|\frac{k}{f}(\rho_1 + \rho_2)\right|\right] \times \exp\left[-\frac{1}{2} \left|\frac{k\sigma}{f}(\rho_1 - \rho_2)\right|^2\right], \quad (11)$$

where  $\gamma = 1/(8\sigma^2) + 1/(2\delta^2)$ ,  $f$  is the focal length of the lens, and  $I_0$  is a zeroth-order modified Bessel function of the first kind. The  $\sigma$ ,  $\delta$ , and  $\beta$  of the BGSM source shown in Fig. 2 were 0.4525 mm, 1.3576 mm, and 10, respectively.

The layout of Fig. 2 is as follows: Figs. 2(a) and 2(b) show the theoretical BGSM source-plane and far-zone  $S$ , respectively. Figures 2(c) and 2(d) show the experimental CS source-plane and far-zone  $S$  results. Figures 2(e) and 2(f) show the experimental MPS source-plane and far-zone  $S$  results. Lastly, Figs. 2(g) and 2(h) show the  $y = 0$  slices of Figs. 2(a), 2(c), and 2(e) and Figs. 2(b), 2(d), and 2(f), respectively. The CS and MPS source-plane and far-zone RMSEs are computed using

$$e = \sqrt{\langle (S^{\text{exp}} - S^{\text{thy}})^2 \rangle}, \quad (12)$$

where  $S^{\text{exp}}$  and  $S^{\text{thy}}$  are the experimental and theoretical spectral densities, respectively, and the mean is computed over all image pixels, as reported in Table 1.

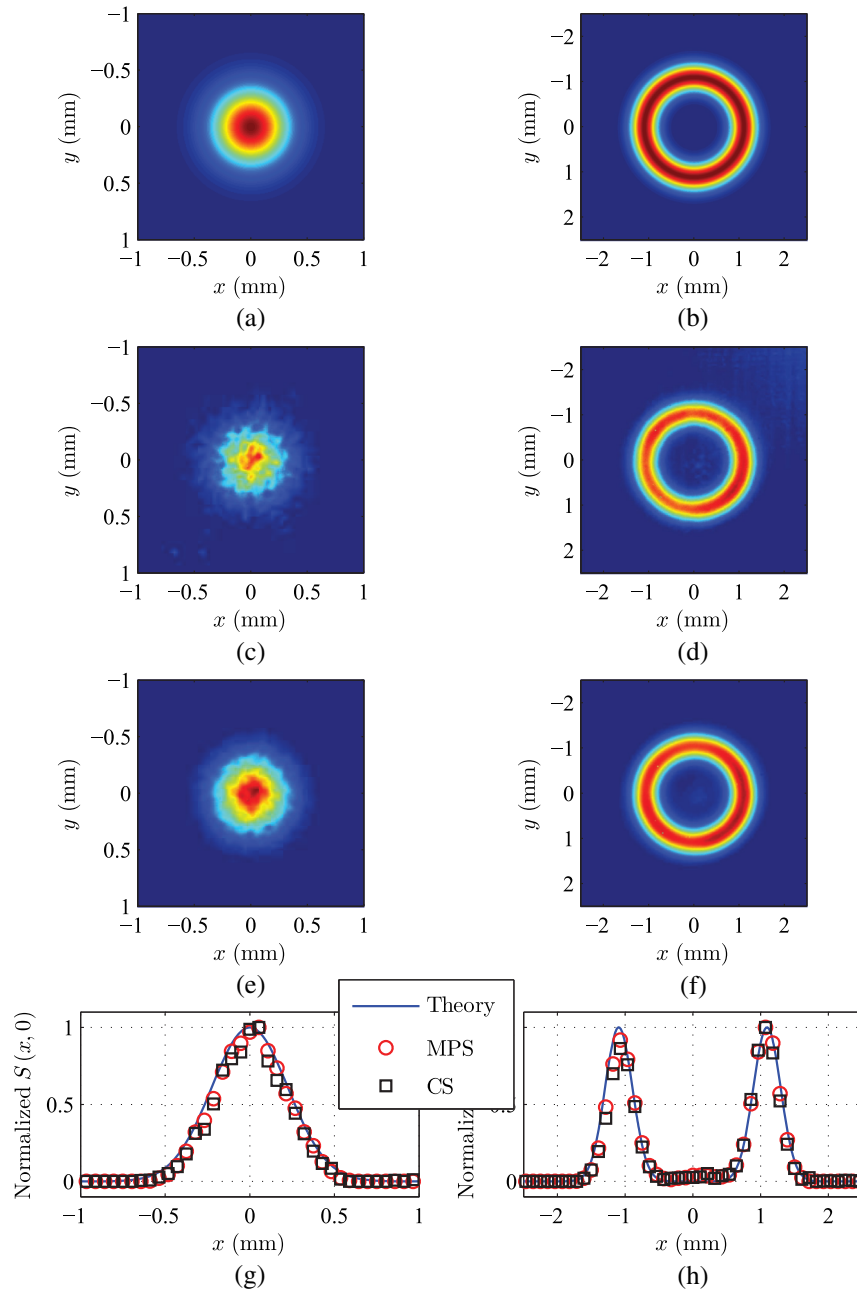


**Fig. 2** Experimental BGSF results—(a) theoretical source-plane  $S$ ; (b) theoretical far-zone  $S$ ; (c) experimental CS source-plane  $S$ ; (d) experimental CS far-zone  $S$ ; (e) experimental MPS source-plane  $S$ ; (f) experimental MPS far-zone  $S$ ; (g)  $y = 0$  slice of theoretical, MPS, and CS experimental normalized source-plane  $S$ ; and (h)  $y = 0$  slice of theoretical, MPS, and CS experimental normalized far-zone  $S$ .

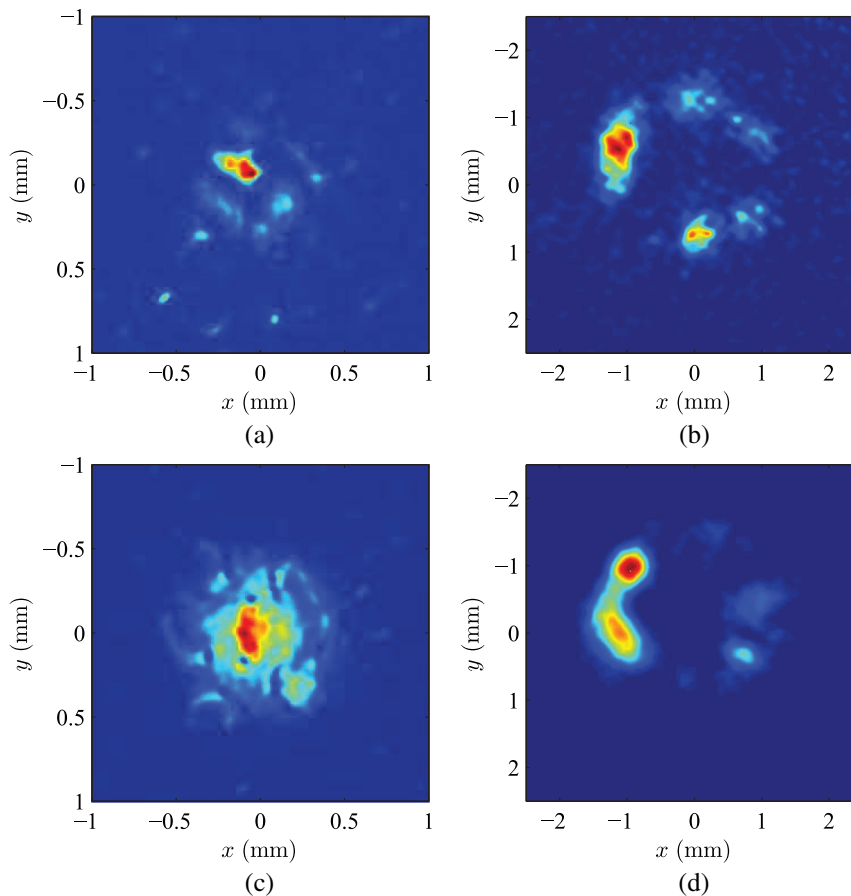
Although the desired Schell-model source can never be exactly reproduced using the MPS method, the agreement between the theoretical and experimental MPS results in Fig. 2 is excellent. Note that the CS and MPS results generally converge to the same source-plane and far-zone  $S$ . However, upon closer inspection, the MPS source-plane and far-zone  $S$  are better developed than their CS counterparts. This qualitative assessment is validated by the RMSEs reported in Table 1, where the MPS results are 1.5 to 2 times more accurate than the corresponding CS results.

Figure 3 provides insight into why the MPS approach outperforms the CS method. The figure shows example single-instance source-plane and far-zone  $|U|^2$  results for the CS

[Figs. 3(a) and 3(b)] and MPS [Figs. 3(c) and 3(d)] methods. Note that the MPS images, qualitatively, are smoother and less speckled than the CS images. This results in faster and more uniform convergence to the desired Schell-model source.

**Table 1** CS and MPS source-plane and far-zone RMSEs  $e$ .

	Source-plane $e$	Far-zone $e$
CS	0.0201	0.0605
MPS	0.0094	0.0400



**Fig. 3** Single instance CS and MPS SPC and FZC images—(a) example CS SPC image, (b) example CS FZC image, (c) example MPS SPC image, and (d) example MPS FZC image.

#### 4 Conclusion

A significant improvement to the CS method, introduced in Ref. 4, was presented. The new technique, called the MPS method, applied a deterministic amplitude and the phase of a CS to an initially coherent light source using a single phase-only SLM. Like the CS approach, the MPS method could generate any desired Schell-model source; however, in contrast with the CS method, it did not produce fully developed speckle patterns in the source plane, resulting in faster and more uniform convergence to the desired partially coherent source.

The analytical development of the MPS method was presented. Included in this development were brief summaries of the CS approach and how amplitude was controlled using a single phase-only SLM. Experimental results of a BGSM source were presented to test the MPS technique. The results convincingly showed the utility of the new method for generating general Schell-model sources.

Like the CS method from which it is derived, the MPS technique will be useful in applications where beam shape and coherence control are important. Some of these applications include particle manipulation, manufacturing, medicine, remote sensing, and directed energy.

#### Acknowledgments

This work was supported by the Air Force Office of Scientific Research (AFOSR) Multidisciplinary Research

Program of the University Research Initiative (MURI) Grant FA9550-12-1-0449. This research was supported in part by an appointment to the Postgraduate Research Participation Program at the Air Force Institute of Technology administered by the Oak Ridge Institute for Science and Education through an interagency agreement between the US Department of Energy and AFIT. The views expressed in this paper are those of the authors and do not reflect the official policy or position of the US Air Force, the Department of Defense, or the US government.

#### References

1. O. Korotkova, *Random Light Beams: Theory and Applications*, CRC, Boca Raton, Florida (2014).
2. Q. Zhan, Ed., *Vectorial Optical Fields: Fundamentals and Applications*, World Scientific, Hackensack, New Jersey (2014).
3. T. J. Santner, B. J. Williams, and W. I. Notz, *The Design and Analysis of Computer Experiments*, Springer-Verlag, New York (2003).
4. M. W. Hyde et al., "Experimentally generating any desired partially coherent Schell-model source using phase-only control," *J. Appl. Phys.* **118**(9), 093102 (2015).
5. M. W. Hyde, IV et al., "Producing any desired far-field mean irradiance pattern using a partially-coherent Schell-model source," *J. Opt.* **17**(5), 055607 (2015).
6. J. W. Goodman, *Speckle Phenomena in Optics: Theory and Applications*, Roberts & Company, Englewood, Colorado (2007).
7. E. Bolduc et al., "Exact solution to simultaneous intensity and phase encryption with a single phase-only hologram," *Opt. Lett.* **38**, 3546–3549 (2013).
8. J. A. Davis et al., "Encoding amplitude information onto phase-only filters," *Appl. Opt.* **38**, 5004–5013 (1999).